Secondary Structure Components and Properties of the Melibiose Permease from *Escherichia coli*: A Fourier Transform Infrared Spectroscopy Analysis

Natàlia Dave,* Agnès Troullier,† Isabelle Mus-Veteau,‡ Mireia Duñach,* Gérard Leblanc,‡ and Esteve Padrós*

*Unitat de Biofísica, Departament de Bioquímica i de Biologia Molecular, Facultat de Medicina, Universitat Autònoma de Barcelona, Bellaterra, Barcelona 08193, Spain; †Laboratoire de Biophysique Moléculaire et Cellulaire, Unité Mixte de Recherche, Centre National de la Recherche Scientifique, Département de Biophysique Moléculaire et Structurale, CEA-Grenoble, 38054 Grenoble 09, France; and ‡Laboratoire de Physiologie des Membranes Cellulaires, Laboratoire de Recherche Correspondant du Commissariat à l'Energie Atomique 16V, Université de Nice Sophia-Antipolis, and Centre National de la Recherche Scientifique (ERS 1253), 06238 Villefranche sur Mer, France

ABSTRACT The structure of the melibiose permease from *Escherichia coli* has been investigated by Fourier transform infrared spectroscopy, using the purified transporter either in the solubilized state or reconstituted in *E. coli* lipids. In both instances, the spectra suggest that the permease secondary structure is dominated by α-helical components (up to 50%) and contains β-structure (20%) and additional components assigned to turns, 3_{10} helix, and nonordered structures (30%). Two distinct and strong absorption bands are recorded at 1660 and 1653 cm^{-1}, i.e., in the usual range of absorption of helices of membrane proteins. Moreover, conditions that preserve the transporter functionality (reconstitution in liposomes or solubilization with dodecyl maltoside) make possible the detection of two separate α-helical bands of comparable intensity. In contrast, a single intense band, centered at ~1656 cm^{-1}, is recorded from the inactive permease in Triton X-100, or a merged and broader signal is recorded after the solubilized protein is heated in dodecyl maltoside. It is suggested that in the functional permease, distinct signals at 1660 and 1653 cm^{-1} arise from two different populations of α-helical domains. Furthermore, the sodium- and/or melibiose-induced changes in amide I line shape, and in particular, in the relative amplitudes of the 1660 and 1653 cm^{-1} bands, indicate that the secondary structure is modified during the early step of sugar transport. Finally, the observation that ~80% of the backbone amide protons can be exchanged suggests high conformational flexibility and/or a large accessibility of the membrane domains to the aqueous solvent.

INTRODUCTION

Melibiose permease (MelB) of *Escherichia coli* couples the uphill transport of α- or β-galactosides to the downhill inward movement of Na^+, Li^+, or H^+. Although MelB is among the best studied transporters of a large family of Na^+ solute symporters (Pourcher et al., 1990; Poolman and Konings, 1993; Reizer et al., 1994), it has become increasingly apparent that both static and dynamic structural information is required to describe how this transporter as well as hundreds of membrane cotransporters (or symporters) use the transmembrane electrochemical potential gradient of ions to drive solute transport in living cells. Purification of the 53-kDa hydrophobic membrane transporter encoded by the MelB gene (Yazu et al., 1984) to homogeneity led to the demonstration that it is solely responsible for the ion-coupled sugar transport activity (Pourcher et al., 1995).

Combinations of experimental manipulation of the different coupling ions and kinetic studies (Pourcher et al., 1990), mutagenesis or chimera constructs, MelB purification (Pourcher et al., 1995), and fluorescence spectroscopic approaches have been used in the past to obtain insights into several aspects of the MelB transport mechanism. Thus it has been proposed that several acidic residues located in membrane domains of the N-terminal half of MelB may form a coordination network involved in ion recognition (Wilson and Wilson, 1992; Hama and Wilson, 1993; Pourcher et al., 1993). It has also been suggested that the sugar-binding site may be preferentially located in the C-terminal half of MelB, and the N and C domains may be close to each other (Wilson and Wilson, 1994; Mus-Veteau et al., 1995; Mus-Veteau and Leblanc, 1996; Cordat et al., 1998; Maehrel et al., 1998). These studies also demonstrated ion-induced cooperative modification of the sugar-binding domain. Many of the above-mentioned conclusions rely on a topological model of MelB consisting of 12 transmembrane domains and with the N and C termini located in the cytoplasm. This model has received strong support from immunological studies (Bottfield and Wilson, 1988), extensive *melB-phoA* fusion analyses (Bottfield et al., 1992; Pourcher et al., 1996), and proteolytic mapping (Gwizdek et al., 1997). Neither the α-helical nature of the MelB membrane domains nor their contribution to the co-substrate-induced conformational change has been documented experimentally.

Fourier transform infrared (FTIR) spectroscopy is a well-established technique for the examination of protein secondary structure and structural changes (Surewicz et al., 1993; Goormaghtigh et al., 1994). Identification of protein secondary structure components and their relative propor-

Received for publication 1 December 1999 and in final form 17 April 2000.

Address reprint requests to Dr. Esteve Padrós, Unitat de Biofísica, Facultat de Medicina, Universitat Autònoma de Barcelona, 08193 Bellaterra, Barcelona, Spain. Tel.: +34-935811870; Fax: +34-935811907; E-mail: esteve.padros@uab.es.

0006-3495/00/08/747/09 $2.00

tion in the overall structure can be derived from an analysis of the protein absorption due to carbonyl stretching vibration of the peptide backbone (appearing in the amide I band), using resolution enhancement and spectral decomposition techniques (Byler and Susi, 1986; Surewicz and Mantsch, 1988; Fabian et al., 1992; Arrondo et al., 1993; Jackson and Mantsch, 1995). Moreover, the effect of substituting D for H atoms in the peptide linkage on the amide II signal provides an insight into the accessibility of the protein backbone to the aqueous solvent.

In the present study, we use FTIR spectroscopy to first identify the structural components of purified MelB reconstituted in proteoliposomes equilibrated in both H_2O and D_2O. The secondary structure in MelB proteoliposomes is then compared to that recorded from active or inactivated MelB transporters in the solubilized state. Finally, evidence suggesting that the interaction of the cosubstrates Na^+ and sugar with MelB modifies the secondary structure of the transporter is presented.

MATERIALS AND METHODS

Materials

p-Nitrophenyl α-D-(6-^{3}H)galactopyranoside ([^{3}H]α-NPG) was synthesized in our department (Laboratoire de Physiologie des Membranes Cellulaires) under the direction of Dr. B. Rousseau. Synthesis of LAPAO ((3-lauryl-amido)-*N,N′*-(dimethylamino)propylamine oxide) was performed as described by Brandolin et al. (1980). Dodecyl maltoside (DM) was obtained from Boehringer Mannheim, and Ni-NTA resin was from Qiagen. SM-2 Bio-Beads were obtained from Bio-Rad. Total *Escherichia coli* lipids (acetone/ether precipitated) were purchased from Avanti Polar Lipids. High purity grade salts or chemicals (Suprapur; Merck) were used to prepare nominally Na^+-free media containing less than 20 mM sodium salts. All other materials were obtained from commercial sources.

MelB overproduction and purification

A RecA^- derivative of *E. coli* DW2 (D*mel* D*lac*ZY) (Bottfield and Wilson, 1988) was transformed with pK95DAHB plasmid to overexpress a wild-type His-tagged MelB (Mus-Veteau and Leblanc, 1996). Transformed cells were grown at 30°C in 200 L of M9 medium supplemented with appropriate carbon sources and ampicillin (100 mg/ml) at the Centre de Fermentation, Centre National de la Recherche Scientifique (Marseille, France), and used to prepare inverted membrane vesicles (IMVs), by means of a French press (American Instrument Co). Purification of the His-tagged MelB was essentially carried out as described by Pourcher et al. (1995).

Preparation of MelB proteoliposomes

MelB protein (0.5 mg/ml) solubilized in dodecyl maltoside (0.1%, w/v) was mixed with *E. coli* lipids to give a protein-to-lipid ratio of 1:2 (w/w). Dodecyl maltoside was removed by an overnight adsorption in SM-2 Bio-Beads at 4°C as described (Rigaud et al., 1988). The proteoliposomes were then subjected to repeated freeze/thaw-sonication-wash cycles in nominally Na^+-free, 0.1 M potassium phosphate buffer (pH 7) to eliminate NaCl from both the external medium and the internal space. For H/D exchange experiments, proteoliposomes were also subjected to repeated freeze/thaw-sonication-wash cycles in sugar and Na^+-free D_2O media (pD 7.4) and then equilibrated for 48 h at 4°C before data collection. When specified, NaCl and/or sugar was added before sonication, using stock solutions prepared in D_2O.

MelB activity and protein assays

MelB activity in proteoliposomes or in the solubilized state was assessed by measuring [α-^{3}H]NPG binding activity (Damiano-Forano et al., 1986). The protein concentration was assayed according to the method of Lowry et al. (1951), using serum bovine albumin as the standard.

Sample preparation and FTIR spectra acquisition

Aliquots of MelB proteoliposomes (~12 mg/ml of protein) in H_2O buffers were briefly sonicated and placed in CaF_2 IR cells fitted with 6-μm tin spacers. Proteoliposomes (13–15 mg/ml protein) equilibrated in D_2O buffer (pD 7.4) were placed in CaF_2 cells fitted with 25-μm Teflon spacers. Solubilized MelB was prepared by concentrating the eluted material to obtain a sample containing 10 mg/ml protein in 0.4% DM (w/w) buffer. FTIR spectra were collected using a Mattson Polaris or a Digilab FTS 6000 spectrometer equipped with an MCT detector, at 2 cm^{-1} resolution. The spectrometer was continuously purged with dry air, and, unless otherwise stated, the sample was maintained at 25°C by means of a thermostatted cell jacket. For each sample, 1000 scans were accumulated, using a sample shuttle to compensate for residual H_2O vapor bands, apodized with a triangle function, and Fourier transformed. The absorption spectra were obtained by digital subtraction of solvent spectra recorded under the same conditions to obtain a straight baseline between 1950 and 1750 cm^{-1}.

Analysis of spectra

Fourier self-deconvolution was performed using the Kauppinen algorithm (Kauppinen et al., 1981) implemented in the FD program (Spectrum Square). The deconvolution parameters generally used in the amide region were a full width at half-height (FWHH) of 14 cm^{-1} and a *k* factor of 2.5–2.7. The *k* values were always kept below log(*S*/*N*) as indicated (Mantsch et al., 1988). A Lorentzian line-shape function and a Bessel apodization function were used. Derivative spectra in the Fourier space were obtained using the Kauppinen algorithm (Kauppinen et al., 1981), using a derivative power of 3 (equivalent to a fourth derivative in the real space) and a breakpoint of 0.2. The spectra were also processed with the maximum likelihood restoration method as described (de Noyer and Dodd, 1991), implemented with the SSRES software (Spectrum Square). Curve fitting was performed with the GRAMS software (Galactic Industries Co.) over deconvoluted spectra. The percentages of the different secondary structures were quantified by a least-square iterative curve fitting procedure implemented in GRAMS software (Galactic Industries Co.), enabling us to fit Gaussian line shapes to the amide I or I′ region of the deconvoluted spectra. The fit was initialized with the number, and band frequencies were obtained by self-deconvolution and derivation. For all of the bands, a 5–7 cm^{-1} FWHH and an intensity of about two-thirds of the spectrum intensity at the same frequency were set. During the fit, only the band frequency was restricted to vary by 2–3 cm^{-1} from the initial value. The proportion of particular structures was calculated from the areas of the fitted Gaussian bands divided by the area of all the bands with maxima between 1685 and 1620 cm^{-1}. For H/D exchange measurements, the percentage of unexchanged protons was estimated by the ratios of band area, $(A_{II}/A_I)D_2O/(A_{II}/A_I)H_2O$. The areas of amide I or I′ and amide II were obtained by integration between 1692 and 1600 cm^{-1}, and 1568 and 1500 cm^{-1}, respectively.

RESULTS

Band characterization of MelB reconstituted in proteoliposomes

His-tagged MelB was purified to homogeneity and reconstituted in liposomes at a lipid-to-protein ratio of 2 (w/w), equivalent to a ratio of 120 (mol/mol). Measurement of the Na^+-dependent [α-^{3}H]NPG binding to the proteoliposomes indicates that at least 70% of the MelB transporters were active.

The infrared absorbance spectrum of MelB proteoliposomes in H_2O buffer recorded in the 1500–1800 cm^{-1} interval is essentially composed of three bands: the lipid ester C═O stretching modes centered at 1741 cm^{-1}, the amide I band at 1657 cm^{-1}, and the amide II band at 1545 cm^{-1} (Fig. 1 *a*). The spectra were first analyzed by a deconvolution method (Fig. 1 *b*), taking care to use a low bandwidth value, to avoid overdeconvolution. Furthermore, a *k* factor well below log (signal/noise) was applied, to avoid noise enhancement, which could give rise to artifactual bands (Kauppinen et al., 1981; Mantsch et al., 1988). As seen, the amide I region is dominated by two major bands appearing at 1660 and 1653 cm^{-1}, respectively, which can be assigned mainly to α-helices, taking into account that some unordered structures can also contribute to the 1653 cm^{-1} band (Byler and Susi, 1986; Surewicz and Mantsch, 1988; Holloway and Mantsch, 1989). The possible significance of two different bands assigned to α-helical structures will be dealt with in the Discussion. Among other individualized bands are those recorded in the region 1669–1685 cm^{-1}, which can mainly be assigned to reverse turns and those appearing in the region 1640–1628 cm^{-1}, which essentially correspond to β-sheets. In the amide II region, the major component at 1547 cm^{-1} confirms the dominant presence of α-helices. Finally, the tyrosine ring band appears at 1516 cm^{-1}. It should be mentioned that the deconvoluted spectrum of the lipid components in the amide region does not show any peak that could interfere with the protein bands. Thus band quantification or changes in band shapes (see below) are not affected by the lipid bands.

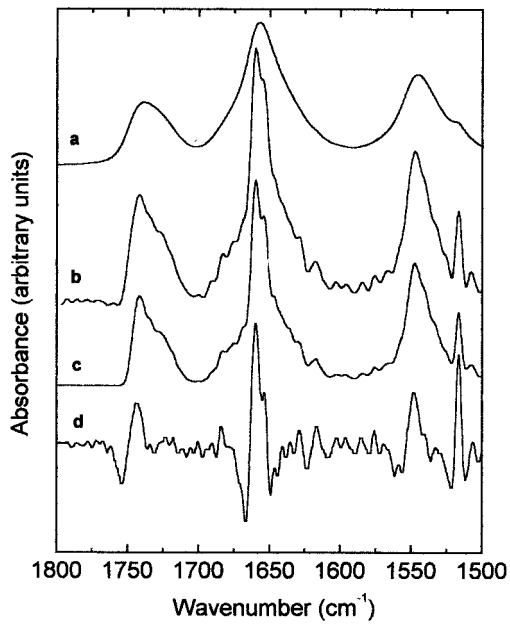

FIGURE 1 FTIR spectra of reconstituted MelB with *E. coli* lipids (1:2 w/w) suspended in 0.1 M potassium phosphate buffer (pH 7.0) at 20°C. (*a*) Absorbance spectrum. (*b*) Deconvoluted trace, obtained using a bandwidth at half-height of 14 cm^{-1} and an enhancement factor of 2.6. (*c*) Maximum likelihood restoration of the absorption spectrum, calculated using a bandwidth at half-height of 14 cm^{-1} and an uncertainty of 0.5%, equivalent to a signal-to-noise ratio of 200. (*d*) Fourier third derivative (equivalent to the fourth derivative in real space) of the absorbance spectrum. The breakpoint used was 0.2.

The MelB absorbance spectra were subjected to additional analysis by two different methods. The first additional method was maximum likelihood restoration. This nonlinear method acknowledges the noise content of the data and estimates the most probable components of the spectrum by looking for the parent set that maximizes the probability of the obtained spectrum (Stephenson, 1988; de Noyer and Dodd, 1991). As shown in Fig. 1 *c*, the maximum likelihood restoration method further confirmed the shape and position of the bands revealed by deconvolution. A second method used was Fourier derivative. As seen in Fig. 1 *d*, the Fourier derivative identifies peaks that show a close correspondence to those revealed by deconvolution or by maximum likelihood restoration.

Fig. 2 compares the spectra recorded from MelB proteoliposomes equilibrated in H_2O or D_2O buffer. Overall, the infrared absorption is slightly shifted to lower wavenumbers after H/D exchange. A major change in absorbance intensity occurs at the level of the amide II region due to the shift of the band from 1550 cm^{-1} to the 1460 cm^{-1} region. In the amide I′ region, bands similar to those described for the H_2O medium are found in both the deconvoluted and derivative spectra of samples in D_2O. This includes two principal peaks at 1660 and 1653 cm^{-1}, which can be assigned to α-helices (Surewicz and Mantsch, 1988; Holloway and Mantsch, 1989; Fabian et al., 1992; Arrondo et al., 1993; Jackson and Mantsch, 1995). This assignment agrees with that determined in H_2O buffer. Finally, the comparison of the amide II/amide I band intensity ratios in H_2O and D_2O indicates that ~80% of the H have been exchanged after 48 h in D_2O medium.

Secondary structure quantification

Fig. 3 *A* shows the amide I deconvoluted spectrum of MelB proteoliposomes in H_2O buffer, along with the best-fitted component bands. This spectrum corresponds to a preparation different from that shown in Fig. 1 and as such can serve as an indication of variability from sample to sample.

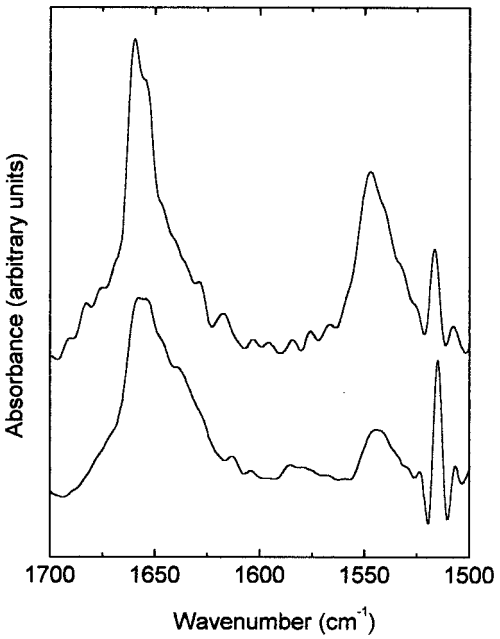

FIGURE 2 Deconvoluted spectra of reconstituted MelB in the amide region. (*Top trace*) Suspended in H_2O buffer (*spectrum b* of Fig. 1). (*Bottom trace*) Suspended in D_2O, 0.1 M potassium phosphate buffer (pD 7.4), at 20°C. The parameters used for deconvolution were the same as in Fig. 1.

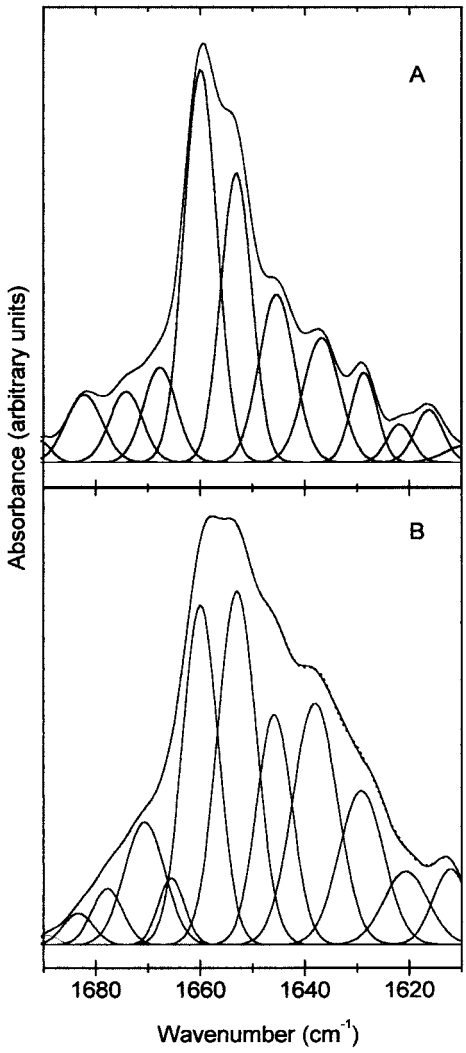

FIGURE 3 Amide I deconvoluted spectra and the best-fitted component bands. (*A*) Reconstituted MelB in H_2O buffer. (*B*) Reconstituted MelB in D_2O buffer.

In general, only small differences are apparent between these spectra, with band analysis revealing a close similarity in between band positions and areas. On the other hand, near-total identity is observed between the original deconvoluted spectrum and the trace resulting from summation of the constituent bands (*discontinuous line*). The areas of these components relative to the whole amide I area and the proposed assignments are listed in Table 1. The bands above 1660 cm^{-1}, assigned to reverse turns, account for ~17% of the total signal. The bands at 1660 and 1653 cm^{-1}, corresponding mainly to α-helices, amount to 32% and 17% of the amide I signal, respectively, together accounting for 49% of the total signal. Interpretation of the band at 1646/1647 cm^{-1}, which accounts for 12%, is more complex. It could arise from either 3_{10} helices (i.e., type III β turns), open loops, or even strongly H-bonded α-helices (Fabian et al., 1992; Arrondo et al., 1993; Surewicz et al., 1993; Jackson and Mantsch, 1995). Finally, the bands between 1640 and 1628 cm^{-1}, assigned mainly to β-sheets, account for 20% of the MelB structure.

Table 1 also lists the MelB structure components deduced from the deconvoluted spectra of MelB proteoliposomes in D_2O buffer (see Fig. 3 *B*). A decrease in the area of component bands located at higher wavenumbers and a corresponding increase in the area of the bands located at lower wavenumbers can be seen. Thus a quantification of ~16% reverse turns (bands at 1683, 1678, 1671, and 1665 cm^{-1}), 42% α-helices (20% for the band at 1660 and 22% for that at 1653 cm^{-1}), and 13% unordered structures plus some α-helical components (band at 1646 cm^{-1}) can be calculated. After H/D exchange, disordered structures can no longer account for the absorbance in the 1660–1650 cm^{-1} interval (Surewicz et al., 1993). The bands at 1638 and 1629 cm^{-1} (29%) can be considered a mixture of β-sheets, 3_{10} helices, and open loops (Fabian et al., 1992; Arrondo et al., 1993; Jackson and Mantsch, 1995).

It has previously been pointed out that quantification of protein secondary structure from spectral deconvolution can suffer from several drawbacks (Holloway and Mantsch, 1989; Arrondo et al., 1993). Although this clearly prevents any precise estimate of the proportion of secondary structure components, spectrum deconvolution gives a trend of their relative importance in the protein structure, preserving qualitative conclusions. It is interesting to note that introduction of the extinction coefficients described by de Jongh

TABLE 1 Secondary structure composition and assignments of *E. coli* melibiose permease

H_2O			D_2O		
Wavenumber* (cm^{-1})	% area*	Assignment	Wavenumber* (cm^{-1})	% area*	Assignment
1683	17	Rev. turns	1683	16	Rev. turns
1676			1678		
1669			1671		
			1665		
1660	49	α, unordered	1660	42	α
1653			1653		
1647	12	3_{10}, open loops, α	1646	13	Unordered, α
1640			1638	29	β-sheets, 3_{10}, open loops
1634	20	β-sheets	1629		
1628					

*These values were rounded off to the nearest integer.

et al. (1996) in our calculation for the sample in H_2O buffer gives 48% α-helices, 12% β-sheets, 26% reverse turns, and 14% other structures, a conclusion that does not question the main trends outlined above.

Structure of solubilized MelB

Fig. 4 (*top trace*) shows the amide I spectrum of MelB solubilized in 0.1% DM, a condition in which the permease retains sugar binding activity (Pourcher et al. 1995). The main bands appear now at 1658 and 1651 cm^{-1}, that is, they are shifted only slightly with respect to the reconstituted MelB in liposomes (see Fig. 1). In addition, other bands appear at slightly different frequencies, reflecting subtle conformational changes when the permease is solubilized in DM. Despite these differences, a native-like secondary structure is preserved upon solubilization in this detergent. Thus the soluble form of MelB has an α-helix content of ~46% (bands at 1658 and 1651 cm^{-1}, although the band at 1651 cm^{-1} may contain some unordered structure). Reverse turns and β-sheets amount to ~24% and ~20%, respectively. The band at ~1645 cm^{-1}, which can be ascribed to a mixture of 3_{10} helices and open loops, accounts for the remaining 10%.

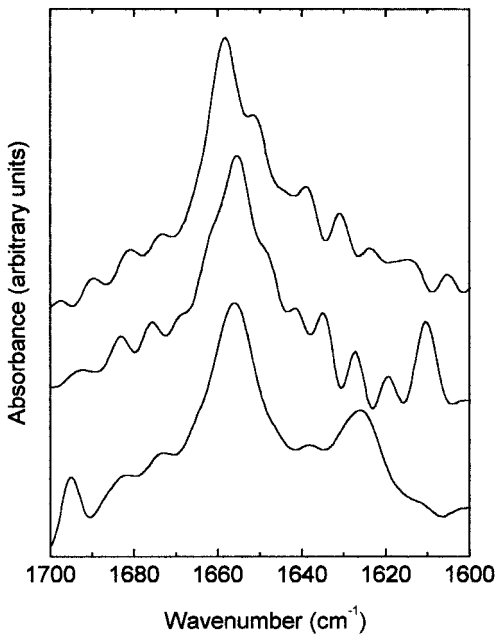

FIGURE 4 Amide I deconvoluted spectra of solubilized MelB in detergent-H_2O buffer. (*Top trace*) In 0.1% DM (w/w). (*Middle trace*) MelB proteoliposomes were solubilized with Triton X-100 (1% w/v). (*Bottom trace*) Solubilized MelB in 0.1% DM after 24 h at 40°C. All absorbance spectra were taken at 4°C and were deconvoluted as indicated in the legend to Fig. 1.

Solubilization of reconstituted MelB in 1% (w/v) Triton X-100 (TX-100), which induces a loss of sugar binding, has a more dramatic effect on the permease structure (Fig. 4, *middle trace*). Thus, as opposed to the double α-helical structure seen in the reconstituted and DM-solubilized samples, the spectrum of MelB in TX-100 contains only one principal α-helical band at 1656 cm^{-1}. This band occupies a position more in the range of standard α-helices. Despite these differences, curve-fitting of MelB in TX-100 leads to similar figures for the secondary content as compared to MelB in DM or after reconstitution. Thus ~46% α-helices (band at 1656 cm^{-1}), 25% reverse turns, 17% β-sheets, and 13% assigned globally to β-sheets, 3_{10} helices, and unordered structures were calculated.

Denaturation of MelB can be accomplished by moderately heating (24 h at 40°C) the solubilized protein in DM. The deconvoluted spectrum (Fig. 4, *bottom trace*) shows the presence of two new bands at 1625 and 1695 cm^{-1}. This result is frequently encountered in the thermal denaturation of proteins and indicates the formation of intermolecular β-sheets arising from aggregation (Clark et al., 1981; Pre-

strelski et al., 1993; Jackson and Mantsch, 1995). The single α-helical band has shifted to 1656 cm^{-1}, the same position as in TX-100. The quantification shows a decrease in the α-helical content to ~37%, with a clear increase of β-sheets to ~36%.

Conformational changes induced by substrate binding

Previous studies of the intrinsic fluorescence properties of MelB strongly suggest that the conformation of the transporter changes upon substrate binding (Mus-Veteau et al., 1995; Mus-Veteau and Leblanc, 1996). The effect of Na^+ and/or melibiose binding to the reconstituted MelB on the FTIR spectra was therefore investigated. As shown in Fig. 5, both substrates elicited significant changes in the IR absorption spectrum, particularly in the bands at 1660 and 1653 cm^{-1} assigned to α-helices. Thus Na^+ binding decreases the intensity of the band at 1653 cm^{-1} and also leads to a slight shift of the main α-helical band at 1660 cm^{-1} to lower wavenumbers. Melibiose binding also decreases the intensity of the band at 1653 cm^{-1} somewhat and shifts the two main bands slightly. This effect was specific for melibiose, as it was not observed when we added saccharose, a poor substrate of MelB. Concomitant binding of Na^+ and melibiose partially reverses the change produced by binding of Na^+ alone. In addition, other changes occurred in the loops and in the β-sheet region.

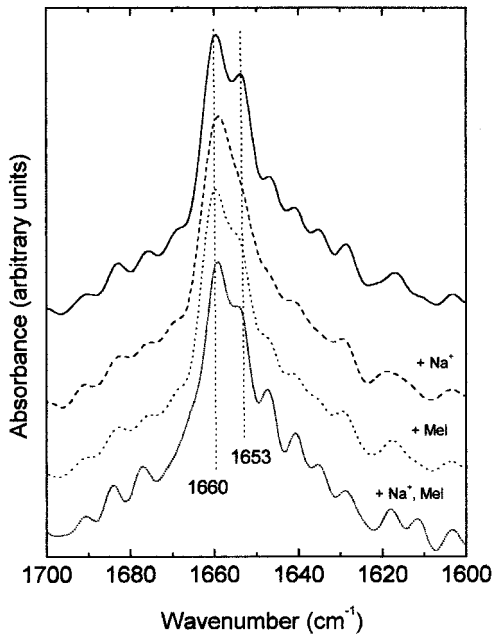

FIGURE 5 Effect of substrates on MelB structure, in H_2O buffer. Shown are the amide I deconvoluted spectra of (*from top to bottom*) reconstituted MelB with *E. coli* lipids (1:2 w/w) suspended in 0.1 M potassium phosphate buffer (pH 7.0), after incubation with 10 mM NaCl, after incubation with 5 mM melibiose; and after incubation with 10 mM NaCl and 5 mM melibiose. All spectra were taken at 20°C and were deconvoluted as indicated in the legend to Fig. 1.

DISCUSSION

The results of the IR spectroscopic analysis of the purified Mel permease from *E. coli* reported above show that MelB secondary structure is dominated by α-helical components and is modified upon substrate binding. Moreover, H/D exchange experiments suggest that most of the MelB structure is accessible to the aqueous solvent.

Strong absorption in the 1660–1651 cm^{-1} interval (amide I mode) and around 1540 cm^{-1} (amide II mode) displayed by membrane proteins is considered to be representative of a high α-helical content (Goormaghtigh et al., 1994; Cabiaux et al., 1997). This holds not only for membrane transporters such as the human erythrocyte glucose transporter (Chin et al., 1986; Alvarez et al., 1987), the lactose permease of *E. coli* (Le Coutre et al., 1997; Patzlaff et al., 1998), and the multidrug antiporter (Arkin et al., 1996), but also for ion or water channels (Mitra et al., 1995; Walz et al., 1995; Cabiaux et al., 1997; Doyle et al., 1998; Le Coutre et al., 1998; Tatulian et al., 1998). The FTIR spectra recorded from the reconstituted and the solubilized MelB also exhibit this typical pattern. Thus the amide I and amide II line shapes of MelB IR absorption spectrum in proteoliposomes equilibrated in H_2O medium are centered around 1657 and 1545 cm^{-1}, respectively, and at 1654 (amide I′) and 1544 cm^{-1} (amide II) after H/D exchange, thus showing that MelB contains a large amount of α-helical structures.

Three independent band-narrowing procedures used (Fourier derivation, deconvolution, and maximum likelihood restoration) indicate that MelB permease displays absorption bands at two distinct frequencies in the 1660–1651 cm^{-1} range, where α-helical components of membrane proteins usually absorb (Holloway and Mantsch, 1989; Fabian et al., 1992; Arrondo et al., 1993; Surewicz et al., 1993; Jackson and Mantsch, 1995). These two bands are still detected after H/D exchange, which suppresses any contribution of unordered structures in this frequency range (Surewicz et al., 1993).

The two bands account for ~40% and ~60%, respectively, of the α-helical signal. This observation contrasts with the inspection of the amide I spectrum of other membrane proteins, including transporters, where only a single component of α-helix was reported (Alvarez et al., 1987; Le Coutre et al., 1997). However, it bears some similarity with the α-helical signal recorded for bacteriorhodopsin, in which two major bands can be distinguished (α_{II} and α_I at 1665 and 1658 cm^{-1}, respectively; Krimm and Dwivedi, 1982; Cladera et al., 1992; Torres et al., 1995). Furthermore, Tatulian et al. (1997) suggested the coexistence of two α-helical components at 1658 and 1650 cm^{-1} in the secretory phospholipase A_2 bound to lipid bilayers, the one at

1658 cm^{-1} corresponding to more flexible and more dynamic α-helices than standard α-helices. It is thus an attractive possibility that the two absorption bands in the 1660–1650 cm^{-1} interval of the MelB spectrum may arise from different α-helical components coexisting in the structure of functional transporters. More support for this view is provided by the observation that these bands can still be identified for the functional solubilized MelB, whereas they cannot be observed for the nonfunctional protein in TX-100 or the denatured and aggregated sample (see Fig. 4). However, we cannot completely discard the possibility that the two distinct bands arise because of protein-protein interactions, or result from the mixture of active (70%) and inactive (30%) permease in the samples analyzed.

Together, the two α-helical populations account for ~50% of the protein structure in H_2O, whether the MelB is reconstituted in proteoliposomes or solubilized. These percentages in H_2O may contain some contribution from unordered structures, but a minimum amount of 42% α-helices can be estimated from MelB proteoliposomes in D_2O, where unordered structures and helix absorption are not overlapping. Moreover, part of the signal recorded around 1647 cm^{-1} may be due to 3_{10} helices or even to α-helices (Venyaminov and Kalnin, 1990). Overall, the data suggest that almost half of the MelB structure consists of α-helical domains, an amount sufficient to build up 12 transmembrane segments. This conclusion is fully compatible with the proposed topological model of MelB consisting of 12 transmembrane α-helical segments (Bottfield et al., 1992; Pourcher et al., 1995). Whether the two α-helical populations absorbing at either 1660 or 1653 cm^{-1} in proteoliposomes could be assigned to different transmembrane helical domains or to different parts of given transmembrane domains remains to be established.

According to our data, the remainder of Mel B structure could be made up of reverse turns (10%), disordered structure (7%), and up to 20% of β domains. Part of the latter could correspond to the 30-amino-acid-long cytoplasmic loop (S206-L234) connecting MelB transmembrane domains X and XI, which are predicted to adopt a β structure conformation (unpublished estimations). However, additional work must be carried out to more clearly ascertain the presence and amount of β domains in MelB.

The observed substrate-induced changes in the line shape of the amide I spectrum and, more precisely, changes in the amplitude of the two major absorbing bands at 1660 and 1653 cm^{-1} suggest a possible modification of the MelB α-helical properties upon interaction of the ion and/or sugar substrates with the transporter. It is worth mentioning that a sugar-induced change in the helical content has previously been reported for the erythrocyte glucose transporter (Chin et al., 1987), although not for Lac permease (Le Coutre et al., 1997). It may be noted that the spectral changes in MelB were different when the two substrates were added separately or together, the largest effect being observed with the addition of the sodium alone and the smallest after the addition of the two substrates. Whether these changes include any term reflecting reorientation of the transporter binding sites across the membrane cannot be stated at the present time. In any event, substrate-dependent modification of the α-helical signal from MelB is not an unexpected finding, in view of previous spectroscopic and biochemical evidence indicating cooperative adjustment of MelB conformation linked to binding of its substrates (Mus-Veteau et al., 1995; Gwizdek et al., 1997; Cordat et al., 1998; Maehrel et al., 1998). Even more so, intrinsic fluorescence studies and fluorescence resonance energy transfer analysis suggest that these changes could arise at the level of helices lining the sugar binding site. One can speculate that the absorption properties of the helical domains bordering the sugar binding site change concomitantly, and this raises the interesting possibility of substrate-induced interconversion of α-helical signals.

Finally, MelB permease shows a high susceptibility to amide hydrogen exchange similar to that of the human erythrocyte glucose transporter or the lactose permease (up to 80%). This estimation may contain some imprecision due to baseline uncertainty and side-chain absorbance overlapping amide I and II bands, but it shows that a majority of the protein backbone is undergoing H/D exchange. A large amount of H/D exchange may reflect the important conformational flexibility of these transporters, which is related to their function as translocators of large hydrophilic sugar substrates (Chin et al., 1986; Alvarez et al., 1987; Le Coutre et al., 1997) or to the presence of water-filled pores or cavities (Tatulian et al., 1998*)*. It can be expected that analysis of the influence of MelB substrates on the kinetic of H/D exchange of the transporter could provide further insight into its tertiary structural properties.

We are grateful to Dr. Joaquim Villaverde for critical reading of the manuscript and to Raymonde Lemonnier for skillful technical assistance.

This work was supported by grant Bio4-CT97-2119 from the European Commission (to GL and EP), grant Picasso 98127 (to GL), and grants PB95-0609 (from the Dirección General de Investigación Científica y Técnica), Secretaría de Estado de Educación, Universidades, Investigación y Desarrollo HF1997-0239, Comisión Interministerial de Ciencia y Tecnología BIO97-1918-CE, and Direcció General de Recerca 1997SGR-31 (to EP). ND is a Ph.D. fellow of the European Commission (Bio4-CT97-2119). AT was supported in part by a fellowship from the Bio-Logic Co. (Claix, France).

REFERENCES

Alvarez, J., D. C. Lee, S. A. Baldwin, and D. Chapman. 1987. Fourier transform infrared spectroscopic study of the structure and conformational changes of the human erythrocyte glucose transporter. *J. Biol. Chem.* 262:3502–3509.

Arkin, I. T., W. P. Russ, M. Lebendiker, and S. Schuldiner. 1996. Determining the secondary structure and orientation of EmrE, a multi-drug transporter, indicates a transmembrane four-helix bundle. *Biochemistry.* 35:7233–7238.

Arrondo, J. L. R., A. Muga, J. Castresana, and F. Goñi. 1993. Quantitative studies of the structure of proteins in solution by Fourier-transform infrared spectroscopy. *Prog. Biophys. Mol. Biol.* 59:23–56.

Bottfield, M. C., K. Naguchi, T. Tsuchiya, and T. H. Wilson. 1992. Membrane topology of the melibiose carrier of *Escherichia coli*. *J. Biol. Chem.* 267:1818–1822.

Bottfield, M. C., and T. H. Wilson. 1988. Mutations that simultaneously alter both sugar cation specificity in the melibiose carrier of *Escherichia coli*. *J. Biol. Chem.* 263:12909–12915.

Brandolin, G., J. Doussiere, A. Gulik, T. Gulik-krzywicki, G. J. Lauquin, and P. V. Vignais. 1980. Kinetic, binding and ultrastructural properties of the beef heart adenine nucleotide carrier protein after incorporation into phospholipid vesicles. *Biochim. Biophys. Acta.* 592:592–614.

Byler, D. M., and H. Susi. 1986. Examination of the secondary structure of proteins by deconvolved FTIR spectra. *Biopolymers.* 25:469–487.

Cabiaux, V., K. A. Oberg, P. Pancoska, T. Walz, P. Agre, and A. Engel. 1997. Secondary structures comparison of aquaporin-1 and bacteriorhodopsin: a Fourier transform infrared spectroscopy study of two-dimensional membrane crystals. *Biophys. J.* 73:406–417.

Chin, J. J., E. K. J. Jung, V. Chen, and C. Y. Jung. 1987. Structural basis of human erythrocyte glucose transporter function in proteoliposome vesicles: circular dichroism measurements. *Proc. Natl. Acad. Sci. USA.* 84:4113–4116.

Chin, J. J., E. K. J. Jung, and C. Y. Jung. 1986. Structural basis of human erythrocyte glucose transporter function in reconstituted vesicles. *J. Biol. Chem.* 261:7101–7104.

Cladera, J., M. Sabés, and E. Padrós. 1992. Fourier transform infrared analysis of bacteriorhodopsin secondary structure. *Biochemistry.* 31: 12363–12368.

Clark, A. H., D. H. P. Saunderson, and A. Suggett. 1981. Infrared and laser Raman spectroscopic studies of thermally induced globular protein gels. *Int. J. Pept. Protein Res.* 17:353–364.

Cordat, E., I. Mus-Veteau, and G. Leblanc. 1998. Structural studies of the melibiose permease of *Escherichia coli* by fluorescence resonance energy transfer. II. Identification of the tryptophan residues acting as energy donors. *J. Biol. Chem.* 273:33198–33202.

Damiano-Forano, E., M. Bassilana, and G. Leblanc. 1986. Sugar binding properties of the melibiose permease in *Escherichia coli* membrane vesicles. Effects of Na^+ and H^+ concentrations. *J. Biol. Chem.* 261: 6893–6899.

de Jongh, H. H. J., E. Goormaghtigh, and J.-M. Ruysschaert. 1996. The different molar absorptivities of the secondary structure types in the amide I region: an attenuated total reflection infrared study on globular proteins. *Anal. Biochem.* 242:95–103.

de Noyer, L. K., and J. G. Dodd. 1991. Maximum likelihood restoration of noisy data. *Am. Lab.* 23:D24.

Doyle, D. A., J. M. Cabral, R. A. Pfuetzner, A. Kuo, J. M. Gulbis, S. L. Cohen, B. T. Chait, and R. Mackinnon. 1998. The structure of the potassium channel: molecular basis of K^+ conduction and selectivity. *Science.* 280:730–732.

Fabian, H., D. Naumann, R. Misselwitz, O. Ristau, D. Gerlach, and H. Welfle. 1992. Secondary structure of streptokinase in aqueous solution: a Fourier transform infrared spectroscopic study. *Biochemistry.* 31: 6532–6538.

Goormaghtigh, E., V. Cabiaux, and J. M. Ruysschaert. 1994. Determination of soluble and membrane protein structure by Fourier transform infrared spectroscopy. I. Assignments and model compounds. *Subcell. Biochem.* 23:329–362.

Gwizdek, C., G. Leblanc, and M. Bassilana. 1997. Proteolytic mapping and substrate protection of the *Escherichia coli* melibiose permease. *Biochemistry.* 36:8522–8529.

Hama, H., and T. H. Wilson. 1993. Cation-coupling in chimeric melibiose carrier derived from *Escherichia coli* and *Klebsiella pneumoniae*. The amino-terminal portion is crucial for Na^+ recognition in melibiose transport. *J. Biol. Chem.* 268:10060–10065.

Holloway, P. W., and H. H. Mantsch. 1989. Structure of cytochrome b5 in solution by Fourier-transform infrared spectroscopy. *Biochemistry.* 28: 931–935.

Jackson, M., and H. H. Mantsch. 1995. The use and misuse of FTIR spectroscopy in the determination of protein structure. *Crit. Rev. Biochem. Mol. Biol.* 30:95–120.

Kauppinen, J. K., D. J. Moffatt, H. H. Mantsch, and D. G. Cameron. 1981. Fourier self-deconvolution: a method for resolving intrinsically overlapped bands. *Appl. Spectrosc.* 35:271–276.

Krimm, S., and A. M. Dwivedi. 1982. Infrared spectrum of the purple membrane: clue to a proton conduction mechanism. *Science.* 216: 407–408.

Le Coutre, J., H. R. Kaback, C. K. N. Patel, L. Heginbothams, and C. Miller. 1998. Fourier transform infrared spectroscopy reveals a rigid alpha-helical assembly for the tetrameric *Streptomyces lividans* K^+ channel. *Proc. Natl. Acad. Sci. USA.* 95:6114–6117.

Le Coutre, J., L. R. Narasimhan, C. K. N. Patel, and H. R. Kaback. 1997. The lipid bilayer determines helical tilt angle and function in lactose permease of *Escherichia coli*. *Proc. Natl. Acad. Sci. USA.* 94: 10167–10171.

Lowry, O. H., N. J. Rosenbrough, A. L. Farr, and R. J. Randall. 1951. Protein measurement with the Folin phenol reagent. *J. Biol. Chem.* 193:265–275.

Maehrel, C., E. Cordat, I. Mus-Veteau, and G. Leblanc. 1998. Structural studies of the melibiose permease of *Escherichia coli* by fluorescence resonance energy transfer. Evidence for ion-induced conformational change. *J. Biol. Chem.* 273:33192–33197.

Mantsch, H. H., D. J. Moffatt, and H. Casal. 1988. Fourier transform methods for spectral resolution enhancement. *J. Mol. Struct.* 173: 285–298.

Mitra, A. K., A. N. van Hoeck, M. C. Wiener, A. S. Verkman, and M. Yeager. 1995. The CHIP28 water channel visualized in ice by electron crystallography. *Nature Struct. Biol.* 2:726–729.

Mus-Veteau, I., and G. Leblanc. 1996. Melibiose permease of *Escherichia coli*: structural organization of cosubstrate binding sites as deduced from tryptophan fluorescence analyses. *Biochemistry.* 35:12053–12060.

Mus-Veteau, I., T. Pourcher, and G. Leblanc. 1995. Melibiose permease of *Escherichia coli*: substrate-induced conformational changes monitored by tryptophan fluorescence spectroscopy. *Biochemistry.* 34:6775–6783.

Patzlaff, J. S., J. A. Moeller, B. A. Barry, and R. J. Brooker. 1998. Fourier transform infrared analysis of purified lactose permease: a monodisperse lactose permease preparation is stably folded, α-helical, and highly accessible to deuterium exchange. *Biochemistry.* 37:15363–15375.

Poolman, B., and W. N. Konings. 1993. Secondary solute transport in bacteria. *Biochim. Biophys. Acta.* 1183:5–39.

Pourcher, T., M. Bassilana, H. K. Sarkar, H. R. Kaback, and G. Leblanc. 1990. The melibiose/Na^+ symporter of *Escherichia coli*: kinetic and molecular properties. *Philos. Trans. R. Soc. Lond. B.* 326:411–423.

Pourcher, T., E. Bibi, H. R. Kaback, and G. Leblanc. 1996. Membrane topology of the melibiose permease of *Escherichia coli* studied by *melB-phoA* fusion analysis. *Biochemistry.* 35:4161–4168.

Pourcher, T., S. Leclerq, G. Brandolin, and G. Leblanc. 1995. Melibiose permease of *Escherichia coli*: large scale purification and evidence that H^+, Na^+, and Li^+ sugar symport is catalyzed by a single polypeptide. *Biochemistry.* 34:4412–4420.

Pourcher, T., M. L. Zani, and G. Leblanc. 1993. Mutagenesis of acidic residues in putative membrane-spanning segments of the melibiose permease of *Escherichia coli*. *J. Biol. Chem.* 268:3209–3215.

Prestrelski, S. J., N. Tedeschi, T. Arakawa, and J. F. Carpenter. 1993. Dehydration-induced conformational transitions in proteins and their inhibition by stabilizers. *Biophys. J.* 65:661–671.

Reizer, J., A. Reizer, and M. H. Saier, Jr. 1994. A functional superfamily of sodium/solute symporters. *Biochim. Biophys. Acta.* 1197:133–166.

Rigaud, J. L., M. T. Paternostre, and A. Bluzat. 1988. Mechanisms of membrane protein insertion into liposomes during reconstitution procedures involving the use of detergents. Incorporation of the light-driven proton pump bacteriorhodopsin. *Biochemistry.* 27:2677–2688.

Stephenson, D. S. 1988. Linear prediction and maximum entropy methods in NMR spectroscopy. *In* Progress in Nuclear Magnetic Resonance Research. J. W. Emsley, J. Feeney, and L. H. Sutcliffe, editors. Pergamon Press, Oxford. 515–626.

Surewicz, W. K., H. H. Mantsch, and D. Chapman. 1993. Determination of protein secondary structure by Fourier transform infrared spectroscopy: a critical assessment. *Biochemistry.* 32:389–394.

Surewicz, W. K., and H. H. Mantsch. 1988. New insight into protein secondary structure from resolution-enhanced infrared spectra. *Biochim. Biophys. Acta.* 952:115–130.

Tatulian, S. A., R. L. Biltonen, and L. K. Tamm. 1997. Structural changes in a secretory phospholipase A_2 induced by membrane binding: a clue to interfacial activation? *J. Mol. Biol.* 268:809–815.

Tatulian, S. A., D. M. Cortes, and E. Perozo. 1998. Structural dynamics of the *Streptomyces lividans* K^+ channel (SKC1): secondary structure characterization from FTIR spectroscopy. *FEBS Lett.* 429:205–212.

Torres, J., F. Sepulcre, and E. Padrós. 1995. Conformational changes in bacteriorhodopsin associated with protein-protein interactions: a functional α_I-α_{II} helix switch? *Biochemistry.* 34:16320–16326.

Venyaminov, Yu. S., and N. N. Kalnin. 1990. Quantitative IR spectrophotometry of peptide compounds in water (H_2O) solutions. II. Amide absorption bands of polypeptides and fibrous proteins in alpha-, beta-, and random coil conformations. *Biopolymers.* 30:1259–1271.

Walz, T., D. Typke, B. L. Smith, P. Agre, and A. Engel. 1995. Projection map of aquaporin-1 determined by electron crystallography. *Nature Struct. Biol.* 2:730–732.

Wilson, D. M., and T. H. Wilson. 1992. Asp-51 and Asp-120 are important for the transport function of the *Escherichia coli* melibiose carrier. *J. Bacteriol.* 174:3083–3086.

Wilson, D. M., and T. H. Wilson. 1994. Transport properties of Asp-51/Glu and Asp-120/Glu mutants of the melibiose carrier of *Escherichia coli. Biochim. Biophys. Acta.* 1190:225–230.

Yazu, H., S. Shiota-Niiya, T. Shimamoto, H. Kanazawa, M. Futai, and T. Tsuchiya. 1984. Nucleotide sequence of the *melB* gene and characteristics of deduced amino acid sequence of the melibiose carrier in *Escherichia coli. J. Biol. Chem.* 259:4320–4326.